Inorg. Chem. **2004**, *43*, 5850–5859

Functionalized Metal Oxide Clusters: Synthesis, Characterization, Crystal Structures, and Magnetic Properties of a Novel Series of Fully Reduced Heteropolyoxovanadium Cationic Clusters Decorated with Organic Ligands—$[MV^{IV}_6O_6\{(OCH_2CH_2)_2N(CH_2CH_2OH)\}_6]X$ (M = Li, X = Cl·LiCl; M = Na, X = Cl·H_2O; M = Mg, X = 2Br·H_2O; M = Mn, Fe, X = 2Cl; M = Co, Ni, X = 2Cl·H_2O)

M. Ishaque Khan,*,† Saadia Tabussum,† Robert J. Doedens,*,‡ Vladimir O. Golub,§ and Charles J. O'Connor§

Department of Biological, Chemical and Physical Sciences, Illinois Institute of Technology, Chicago, Illinois 60616, Department of Chemistry, University of California, Irvine, California 92697, and Department of Chemistry, University of New Orleans, New Orleans, Louisiana 70148

Received May 4, 2004

A novel series of fully reduced heteropolyoxovanadium(IV) compounds, $[MV^{IV}_6O_6\{(OCH_2CH_2)_2N(CH_2CH_2OH)\}_6]X$ (**1**, M = Li, X = Cl·LiCl; **2**, M = Na, X = Cl·H_2O; **3**, M = Mg, X = 2Br·H_2O; **4**, M = Mn, X = 2Cl; **5**, M = Fe, X = 2Cl; **6**, M = Co, X = 2Cl·H_2O; **7**, M = Ni, X = 2Cl·H_2O), have been synthesized and characterized by FT-IR and UV–vis spectroscopies, thermogravimetric analysis, elemental analysis, manganometric titration, temperature-dependent magnetic susceptibility measurements, bond valence sum calculations, X-ray powder diffraction, and single-crystal X-ray diffraction analyses. The structures of the crystals are comprised of discrete units of fully reduced cluster cations, $[MV^{IV}_6O_6\{(OCH_2CH_2)_2N(CH_2CH_2OH)\}_6]^{n+}$, counterions (chloride or bromide), and water of crystallization (in the case of **2**, **3**, **6**, **7**). In each case the cluster ion is composed of a fully reduced cyclic $\{MV_6N_6O_{18}\}$ (M = Li, Na, Mg, Mn, Fe, Co, Ni) framework decorated with six triethanolamine ligands. Two arms of each triethanolamine ligand are coordinated to the metallacycle, and the third arm projects outward from the hexagonal ring. The $\{MV_6N_6O_{18}\}$ core adopts the Anderson-type structure. The cyclic core is comprised of a ring of six edge-sharing $\{VO_5N\}$ octahedra linked to a central $\{MO_6\}$ unit. The hexametalate ring contains six d^1 ions $\{V^{IV}\}$ and shows remarkable flexibility to encapsulate a variety of metal centers M^{n+} (M^{n+} = Li^+, Na^+, Mg^{2+}, Mn^{2+}, Fe^{2+}, Co^{2+}, Ni^{2+}) with different (d^n) spins. The compounds show good thermal stability and exhibit interesting magnetic properties that make these magnetic clusters promising building blocks for constructing supramolecular structures and extended structure magnetic solids. Crystal data for **1**; $C_{36}H_{78}Cl_2N_6Li_2O_{24}V_6$, trigonal space group $R\bar{3}$, a = 13.7185(3) Å, c = 24.8899(8) Å, Z = 3. Crystal data for **2**: $C_{36}H_{80}ClN_6NaO_{25}V_6$, triclinic space group $P\bar{1}$, a = 11.1817(5) Å, b = 12.1612(5) Å, c = 21.5979(10) Å, α = 75.8210(10), β = 78.8270(10), γ = 71.1400(10), Z = 2. Crystal data for **4**: $C_{36}H_{78}Cl_2N_6MnO_{24}V_6$, monoclinic, space group $P2_1$, a =11.2208(5) Å, b = 21.5041(9) Å, c = 11.8126(5), β = 111.2680, Z= 2. Crystal data for **5**: $C_{36}H_{78}Cl_2N_6FeO_{24}V_6$, monoclinic, space group $P2_1$, a = 11.3057(7) Å, b = 21.4372(13) Å, c = 11.8167(7) Å, β = 111.4170, Z = 2.

Introduction

Vanadium oxide clusters and their coordination compounds represent an expanding subclass of metal oxide clusters (or poloxometalates).[1–4] They are of current interest due mainly to their relevance to catalysis and biochemical

* Authors to whom correspondence should be addressed. E-mail: Khan@iit.edu (M.I.K.); Rdoedens@uci.edu (R.J.D.).
† Illinois Institute of Technology.
‡ University of California
§ University of New Orleans.

(1) Pope, M. T. *Heteropoly and Isopoly Oxomatalates*; Springer-Verlag: New York, 1983.
(2) *Polyoxometalates: From Platonic Solids To Anti-Retroviral Activity*; Pope, M. T., Müller A., Eds.; Academic Press: Dordrecht, 1994; (b) Gatteschi, D.; Pardi, L.; Barra, A.-L.; Müller, A. In *Polyoxometalates: From Platonic Solids to Anti-retroviral Activity*; Pope, M. T., Müller A., Eds.; Kluwer Academic Publishers: Dordrecht, 1994; p 219.

10.1021/ic049417m CCC: $27.50
Published on Web 08/25/2004

systems, their variable geometries, and their redox properties.[1,3−7] The fascinating rich magnetochemistry associated with many of these clusters, especially in their reduced forms, is significant in the context of molecular magnetism—an area of contemporary interest. Magnetic clusters, which can be considered as tiny magnets, are of interest due mainly to their relevance to molecular magnetism.[8−12] Magnetic metal oxide clusters are considered a promising class of chemical systems that offers the opportunity of designing well-defined molecular magnetic systems.[2b,4b] Such clusters can behave as ligands to encapsulate a variety of magnetic metal centers and their clusters, giving rise to systems that can contain different numbers of unpaired spins. Since their sizes can be varied incrementally from discrete molecules to nanometer-size aggregates to infinite solids,[13,14] they provide potential building blocks for preparing tailor-made magnets.[1,4,8,15,16]

The functionalization of metal oxide clusters with organic ligands would further expand their overall application as building blocks for materials design and development. Progress in this direction can pave the way for connecting oxometallic clusters with organic and biological systems (enzymes, cells, and proteins). Functionalized clusters are conceptually attractive molecular building blocks. They can be employed for designing hybrid materials, including optically active ones, and prove useful in designing novel chemical systems for possible applications in chemical and biological sensing.

We are currently exploring the chemistry of vanadium oxide clusters and their derivatives. During the course of this ongoing investigation[17] we found that while numerous compounds of molybdenum and tungsten containing hexametalate cores exhibiting the Anderson structure[18] are known,[1,6,7,19] the corresponding structure based on the hexavanadate core is rare. Moreover, the vast majority of reported polyoxometalate clusters are anionic, and a small number of them are neutral.[20] We have now discovered a novel series of cationic heteropolyoxovanadium(IV) clusters containing a previously unobserved fully reduced metallacyclic core—$\{MV_6N_6O_{18}\}$—exhibiting the Anderson structure and functionalized with triethanolamine ligands. This report describes the hydrothermal synthesis, magnetic properties, and characterization by FT-IR and UV−vis spectroscopies, thermogravimetric analysis, elemental analysis, manganometric titration, temperature-dependent magnetic susceptibility measurements, bond valence sum calculations, X-ray powder diffraction, and single-crystal X-ray diffraction analysis of the following new series of compounds:

$[Li{V^{IV}}_6O_6\{(OCH_2CH_2)_2N(CH_2CH_2OH)\}_6]Cl\cdot LiCl$ (**1**),
$[Na{V^{IV}}_6O_6\{(OCH_2CH_2)_2N(CH_2CH_2OH)\}_6]Cl\cdot H_2O$ (**2**),
$[Mg{V^{IV}}_6O_6\{(OCH_2CH_2)_2N(CH_2CH_2OH)\}_6]2Br\cdot H_2O$ (**3**),
$[Mn^{II}{V^{IV}}_6O_6\{(OCH_2CH_2)_2N(CH_2CH_2OH)\}_6]2Cl$ (**4**),
$[Fe^{II}V_6O_6\{(OCH_2CH_2)_2N(CH_2CH_2OH)\}_6]2Cl$ (**5**),
$[Co^{II}{V^{IV}}_6O_6\{(OCH_2CH_2)_2N(CH_2CH_2OH)\}_6]2Cl\cdot H_2O$ (**6**),
$[Ni^{II}{V^{IV}}_6O_6\{(OCH_2CH_2)_2N(CH_2CH_2OH)\}_6]2Cl\cdot H_2O$ (**7**).

Experimental Section

Materials and Physical Measurements. Commercially available reagent-grade chemicals were purchased from Sigma-Aldrich, Fischer, Cerac, and Alfa Aesar. These were used in experiments without any further purification. The ammonium decavanadate and tetrabutylammonium decavanadate salts were prepared according to the literature methods.[21] All synthesis reactions were carried out in 23-mL Parr Teflon lined acid digestion bombs.

Infrared spectra of the compounds were recorded on a Thermonicolet Nexus 470 Infrared Spectrometer (KBr pellets in 400−4000 cm^{-1} region). The spectra were evaluated using Thermonicolet's OMNIC software. The thermogravimetric analyses of the compounds were performed on a Mettler-Toledo TGA/SDTA 851E instrument, and the results were analyzed using METTLER TOLEDO STAR^e 7.01 Software. Typically, 8−12 mg of the sample was placed in a 70-μL alumina pan and heated in the temperature range 25−800 °C at a rate of 5 °C/min in a nitrogen atmosphere with a flow rate of 60−90 mL/min.

The magnetic data were recorded on 54.84, 43.48, 34.86, 31.20, 41.46, 28.90, and 37.74 mg of polycrystalline samples of

(3) *Polyoxometalate Chemistry. From Topology via Self-Assembly to Applications*; Pope, M. T., Müller, A., Eds.; Kluwer Academic Publishers: Dordrecht, 2001.
(4) Hill, C. L. (Guest Ed.) See a special edition on ''Polyoxometalates". *Chem. Rev.* **1998**, *98*, 1 (b) Müller, A.; Peters, F.; Pope, M. T.; Gatteschi, D.; Polyoxometalates: very large clusters-nanoscale magnets. *Chem. Rev.* **1998**, *98*, 239.
(5) *Vanadium Compounds: Chemistry, Biochemistry and Therapeutic Applications*; Tracey, A. S., Crans, D. C., Eds.; ACS Symposium Series 711; American Chemical Society: Washington, D.C., 1998. (b) *Vanadium in Biological systems*; Chasteen, N. D., Ed.; Kluwer Academic Publishers: Dordrecht, 1990.
(6) *Polyoxometalate Chemistry. From Topology via Self-Assembly to Applications*; Pope, M. T., Müller, A., Eds.; Kluwer Academic: Dordrecht, 2001.
(7) Pope, M. T.; Müller, A. *Angew. Chem., Int. Ed.* **1991**, *30*, 34. (b) *Polyoxometalates: From Platonic Solids To Anti-Retroviral Activity*; Pope, M. T., Müller, A., Eds.; Kluwer Academic: Dordrecht, 1994. (c) Hill, C. L. (Guest Ed.) See a special edition on "Polyoxometalates". *Chem. Rev.* **1998**, *98*, 1.
(8) Kahn, O. *Molecular Magnetism*; VCH: Weinheim, 1993.
(9) Caneschi, A.; Gatteschi, D.; Sessoli, R. *Acc. Chem. Res.* **1989**, *22*, 392.
(10) Gatteshi, D.; Caneschi, A.; Pardi, L.; Sessoli, R. *Science* **1994**, *265*, 1054.
(11) Sessoli, R.; Gatteshi, D.; Caneschi, A.; Novak, M. A. *Nature* **1993**, *365*, 141.
(12) Tamaki, H.; Zhong, Z. J.; Matsumoto, N.; Kida, S.; Koikawa, M.; Achiwa, N.; Hashimoto, Y.; Okawa, H. *J. Am. Chem. Soc.* **1992**, *114*, 6974. (b) In *Magnetic Molecular Materials*; Gatteshi, D., Kahn, O., Miller, J. S., Palacio, F., Eds.; NATO ASI Series E, 198; Kluwer Academic Publishers: Dordrecht, 1991.
(13) Müller, A.; Kögerler, P.; Kuhlmann, C. *Chem. Commun.* **1999**, *15*, 1347.
(14) Khan, M. I.; Yohannes, E.; Doedens, R. J.; Tabussum, S.; Cevik, S.; Manno, L.; Powell, D. *Cryst. Eng.* **1999**, *2*, 171.
(15) Coronado, E.; Gomez-Garcia, C. J. *Comments Inorg. Chem.* **1995**, *17*, 255.
(16) Awschalom, D. D.; DiVincenzo, D. P.; Smyth, J. F. *Science* **1992**, *258*, 414.
(17) Khan, M. I.; Tabussum, S.; Doedens, R. J. *Chem. Commun*. **2003**, 532. (b) Khan, M. I.; Tabussum, S.; Doedens, R. J.; Golub, V. O.; O'Connor, C. J. *Inorg. Chem. Commun.* **2004**, *7*, 54. (c) Khan, M. I.; Cevik, S.; Doedens, R. J. *Chem. Commun.* **2001**, 1930. (d) Khan, M. I. *J. Solid State Chem.* **2000**, *152*, 105. (e) Khan, M. I.; Yohannes, E.; Doedens, R. J. *Angew. Chem., Int. Ed.* **1999**, *38*, 1292.
(18) Anderson, J. S. *Nature* **1937**, *140*, 850.
(19) Evans, H. T. *J. Am. Chem. Soc*. **1948**, *70*, 1291. (b) Evans, H. T. *Acta Crystallogr., Sect. B* **1974**, *30*, 2095.
(20) Golhen, S.; Ouahab, L.; Grandjean, D.; Molinie, P. *Inorg. Chem*. **1998**, *37*, 1499. (b) Hasenknopf, B.; Delmont, R.; Herson, P.; Gouzerh, P. *Eur. J. Inorg. Chem*. **2002**, 1081.
(21) Klemperer, W. G. *Inorg. Synth.* **1990**, *27*, 71. (b) Evans, H. T., Jr. *Inorg. Chem.* **1966**, *5*, 967.

$[LiV_6O_6\{(OCH_2CH_2)_2N(CH_2CH_2OH)\}_6]Cl\cdot LiCl$, $[NaV_6O_6\{(OCH_2CH_2)_2N(CH_2CH_2OH)\}_6]Cl\cdot H_2O$, $[MgV_6O_6\{(OCH_2CH_2)_2N(CH_2CH_2OH)\}_6]2Br\cdot H_2O$, $[Mn^{II}V_6O_6\{(OCH_2CH_2)_2N(CH_2CH_2OH)\}_6]2Cl$, $[Fe^{II}V_6O_6\{(OCH_2CH_2)_2N(CH_2CH_2OH)\}_6]2Cl$, $[CoV_6O_6\{(OCH_2CH_2)_2N(CH_2CH_2OH)\}_6]2Cl\cdot H_2O$, and $[NiV_6O_6\{(OCH_2CH_2)_2N(CH_2CH_2OH)\}_6]2Cl\cdot H_2O$ in the 2−300 K temperature range using a Quantum Design MPMS-5S SQUID spectrometer. The temperature-dependent magnetic data were obtained at a magnetic field $H = 1000$ O_e. Calibrating and operating procedures were done according to the literature method.[22]

Synthesis. $[LiV_6^{IV}O_6\{(OCH_2CH_2)_2NCH_2CH_2OH\}_6]Cl\cdot LiCl$ (1). To a mixture of $[NH_4]_6[V_{10}O_{28}]\cdot 6H_2O$ (0.136 mmol) and LiCl (1.014 mmol) contained in a 23-mL Teflon vessel, CH_3CN (57.36 mmol), C_2H_5OH (34.305 mmol), and $\{C_2H_4OH\}_3N$ (4.37 mmol) were added. The Teflon vessel was then sealed in a stainless steel Parr autoclave and heated in a Thermoline furnace maintained at 145 °C for 67 h. The reaction vessel was cooled to room temperature for 12 h. The yellowish-green solution was decanted, and the crystalline material on the side and bottom of the Teflon vessel was washed with three 2 mL portions of ethanol. Then crystals were slowly scraped off with a spatula and washed again with five 2 mL portions of ethanol or until no further black impurity was seen in the supernatant solution. The rectangular blue crystals were removed from the Teflon vessel and air dried at room temperature. Any further impurities present in the crystalline product were mechanically removed. The dark blue crystals were obtained in 98.35% yield (based on vanadium). Anal. Calcd for $Li_2V_6O_{24}C_{36}H_{78}N_6Cl_2$: Li, 1.01; V, 22.32; C, 31.57; H, 5.74; N, 6.14; Cl, 5.18. Found: Li, 0.48; V, 22.97; C, 31.72; H, 5.85; N, 6.40; Cl, 3.03. Prominent IR bands (KBr pellet 400−4000 cm^{-1}): 462(s), 481(s), 505(vs), 643(s), 662(vs), 670(vs), 749(s), 901(s), 944(vs), 961(vs), 997(s), 1025(s), 1049(m), 1076(vs), 1087(vs), 1159(m), 1218(m), 1249(m), 1295(m), 1434(s), 1463(s), 2859(vs), 2923(m), 2966(sh), 3368(vs).

$[NaV_6^{IV}O_6\{(OCH_2CH_2)_2NCH_2CH_2OH\}_6]Cl\cdot H_2O$ (2). The sodium derivative (**2**) was synthesized from a reaction mixture of $[NH_4]_6[V_{10}O_{28}]\cdot 6H_2O$ (0.0684 mmol), NaCl (0.17 mmol), CH_3CN (57.36 mmol), C_2H_5OH (51.46 mmol), and $\{C_2H_4OH\}_3N$ (2.38 mmol) sealed in a 23-mL Teflon-lined stainless steel Parr reaction vessel. The vessel was heated in a Thermoline furnace at 145 °C for 24 h, then cooled to room temperature, and opened after 12 h. The yellowish-green solution was decanted, and the crystals were washed with ethanol and air dried according to the procedure described for the synthesis of **1**. Any further white crystalline impurities mixed with the crystalline product were mechanically removed. The blue hexagonal crystals were obtained in 97.5% yield (based on vanadium). Anal. Calcd for $NaV_6O_{25}C_{36}H_{80}N_6Cl$: Na, 1.69; V, 22.46; C, 31.78; H, 5.92; N, 6.17; Cl, 2.60. Found: Na, 1.73; V, 22.52; C, 31.83; H, 6.37; N, 6.29; Cl, 1.77. Prominent IR bands (KBr pellet 400−4000 cm^{-1}): 459(vs), 500(vs), 551(m), 610(vs), 637(vs), 654(vs), 680(m), 749(vs), 904(s), 928(m), 944(vs), 966(vs), 996(vs), 1024(vs), 1051(s), 1071(s), 1088(vs), 1158(m), 1218(s), 1251(s), 1296(s), 1314(s), 1431(s), 1460(s), 1621(s), 2856(s), 3385(vs). UV−vis (190−800 nm region; aqueous solution); λ_{max}, nm (ϵ, L $M^{-1}cm^{-1}$): 240 ($\epsilon = 6.17 \times 10^3$), 252 ($\epsilon = 5.29 \times 10^3$), 248 ($\epsilon = 5.78 \times 10^3$), 224 ($\epsilon = 4.95 \times 10^2$), 234 ($\epsilon = 5.71 \times 10^3$), 218 ($\epsilon = 4.82 \times 10^2$), 208 ($\epsilon = 4.45 \times 10^3$), 628 ($\epsilon = 1.85 \times 10^2$).

$[Mg^{II}V_6^{IV}O_6\{(OCH_2CH_2)_2NCH_2CH_2OH\}_6]2Br\cdot H_2O$ (3). Method I: A Teflon-lined Parr acid digestion bomb was charged sequentially with $MgBr_2\cdot 6H_2O$ (0.147 mmol), $[(n\text{-}C_4H_9)_4N]_3[H_3V_{10}O_{28}]$ (0.05 mmol), CH_3CN (57.4 mmol), C_2H_5OH (34.24 mmol), and $(HOCH_2CH_2)_3N$ (1.9 mmol). The reaction mixture was heated in a Thermoline furnace maintained at 155 °C for 66 h and cooled to room temperature. After 12 h the blue crystals of **3** were washed according to the procedure described in the preparation of **1** until the decanted supernatant solution did not contain any amorphous white impurity. The blue crystals obtained in 44% yield (0.055 g, based on vanadium) were air dried, and any amorphous white impurity was removed mechanically. Compound **3** can also be prepared in high yield, albeit at the cost of crystal quality, by the following synthetic method.

Method II: This method for the preparation of the magnesium derivative (**3**) is similar to the above method I except that $[NH_4]_6[V_{10}O_{28}]\cdot 6H_2O$ (0.0504 mmol) was used instead of $[(n\text{-}C_4H_9)_4N]_3[H_3V_{10}O_{28}]$ in the reaction mixture and the Teflon-lined Parr reaction vessel was heated for 72 h at 155 °C. The light blue thin crystals obtained along with a small amount of white amorphous material were filtered, washed with ethanol, and air dried. Any further impurities in the crystalline product were removed mechanically to give 0.085 g of pure solid. Yield: 68% (based on vanadium). Anal. Calcd for $MgV_6O_{25}C_{36}H_{80}N_6Br_2$: Mg, 1.63; V, 20.32; C, 29.88; H, 5.42; N, 5.65; Br, 10.74. Found: Mg, 2.15; V, 20.32; C, 30.69; H, 5.75; N, 5.96; Br, 6.48. Prominent IR bands (KBr pellet 400−4000 cm^{-1}): 418(s), 442(s), 486(m), 508(vs), 556(s), 648(m), 671(vs), 751(vs), 900(vs), 922(m), 948(sh), 969(s), 996(m), 1018(s), 1154(m), 1221(m), 1243(m), 1303(s), 1350(s), 1384(m), 1395(m), 1435(m), 1440(s), 1462(s), 1617(s), 2870(s), 2923(s), 3355(vs).

$[Mn^{II}V_6^{IV}O_6\{(OCH_2CH_2)_2NCH_2CH_2OH\}_6]2Cl$ (4). $[NH_4]_6[V_{10}O_{28}]\cdot 6H_2O$ (0.0684 mmol), $MnCl_2\cdot 4H_2O$ (0.15 mmol), CH_3CN (57.42 mmol), C_2H_5OH (34.24 mmol), and $(HOCH_2CH_2)_3N$ (1.9 mmol) were placed in a 23-mL Teflon-lined Parr acid digestion bomb and heated at 145 °C in a Thermoline oven for 24.5 h. The reaction vessel was cooled to room temperature and opened after 12 h. The transparent pale yellowish-green solution was decanted, and the crystalline material in the Teflon vessel was washed with three 2 mL portions of ethanol. The crystals were scraped from the bottom and sides of the vessel and washed again with ethanol. The thin light blue hexagonal crystals obtained were air dried to give a high yield (80% based on vanadium) of **4**. Anal. Calcd for $MnV_6O_{24}C_{36}H_{78}N_6Cl_2$: Mn, 3.89; V, 21.67; C, 30.66; H, 5.57; N, 5.96; Cl, 5.03. Found: Mn, 3.74; V, 22.52; C, 30.4; H, 5.5; N, 6.2; Cl, 5.09. Prominent IR bands from blue crystals (KBr pellet 400−4000 cm^{-1}): 429(s), 507(vs), 551(s), 620(sh), 668(vs), 749(s), 900(s), 922(m), 973(vs), 1018(s), 1058(vs), 1088(vs), 1155(m), 1222(m), 1241(m), 1300(m), 1351(m), 1436(s), 1460(s), 2873(vs), 2924(vs), 2942(sh), 2970(sh), 3324(vs).

$[Fe^{II}V^{IV}_6O_6\{(OCH_2CH_2)_2N(CH_2CH_2OH)\}_6]2Cl$ (5). Method I: A mixture of ammonium decavanadate hexahydrate (0.0504 mmol), ferric chloride hexahydrate (0.37 mmol), acetonitrile (57.42 mmol), ethanol (51.4 mmol), and triethanolammine (1.13 mmol) was heated in a Teflon-lined Parr autoclave for 89 h at 145 °C. The reaction vessel was cooled to room temperature for 12−24 h. The brown filtrate was decanted, and the crystalline material that was deposited on the side and bottom of the reaction vessel was washed with ethanol (3 × 2 mL). The crystals were carefully scraped with a spatula and washed again with ethanol (5 × 2 mL) to remove the black- and brown-colored impurity. The bright green diamond-shaped crystals were dried in air at room temperature, and the remaining traces of the impurity were removed mechanically. Yield: ∼63% (based on vanadium). The following modified

(22) O'Connor, C. J. *Prog. Inorg. Chem.* **1979**, *29*, 203. (b) Orbach, R. *Phys. Rev.* **1959**, *115*, 1181.

synthetic method gives **5** in monophasic form and in high yield, albeit at the cost of crystal quality.

Method II: The reaction was carried out in a manner similar to that described above except that 0.0684 mmol (instead of 0.0504 mmol) of ammonium decavanadate hexahydrate and 1.9 mmol (instead of 1.13 mmol) of triethanolamine were used and the reaction mixture was heated for 72 h. The dark green chunky polycrystals of high purity (nearly monophasic form) were filtered from the mother liquor and dried in air at room temperature. Yield: ~93% (based on vanadium). Anal. Calcd for $C_{36}H_{78}Cl_2FeN_6O_{24}V_6$: C, 30.64; H, 5.56; N, 5.94; Cl, 5.02; Fe, 3.96; V, 21.61. Found: C, 29.88; H, 5.72; N, 6.19; Cl, 6.01; Fe, 3.90; V, 21.45. Prominent FT-IR absorption bands for **5** (KBr pellet 1600−400 cm^{-1}): 1461(s), 1437(s), 1351(m), 1309(m), 1297(m), 1242(m), 1087(vs), 1060(vs), 1018(m), 972(vs), 926(s), 899(s), 750(s), 671(s), 665(s), 556(s), 508(s), 435(s). UV−vis (190−800 nm region; aqueous solution); λ_{max}, nm (ϵ, L $M^{-1}cm^{-1}$): 244 ($\epsilon = 6.26 \times 10^3$), 312 ($\epsilon = 3.43 \times 10^3$), 598 ($\epsilon = 2.27 \times 10^2$).

$[Co^{II}V^{IV}_6O_6\{(OCH_2CH_2)_2N(CH_2CH_2OH)\}_6]2Cl\cdot H_2O$ (6). The cobalt derivative **6** was synthesized from a mixture consisting of $[NH_4]_6[V_{10}O_{28}]\cdot 6H_2O$ (0.0684 mmol), $CoCl_2\cdot 6H_2O$ (0.27 mmol), CH_3CN (57.416 mmol), C_2H_5OH (51.396 mmol), and $(HOCH_2CH_2)_3N$ (1.9 mmol). The reaction mixture was sealed in a 23-mL Teflon-lined Parr reaction vessel and heated in a Thermoline oven at 145 °C for 60 h. The reaction vessel was cooled to room temperature for 12 h. The dark brown solution was decanted, and blue thin crystals clumped together were separated. The crystals were washed with ethanol and air dried at room temperature. Any impurity was mechanically removed to give crystalline product in 84.68% yield (based on vanadium). Anal. Calcd for $CoV_6O_{25}C_{36}H_{80}N_6Cl_2$: Co, 4.11; V, 21.34; C, 30.18; H, 5.63; N, 5.87; Cl, 4.95. Found: Co, 4.20; V, 21.37; C, 30.01; H, 5.59; N, 5.90; Cl, 4.98. Prominent IR bands (KBr pellet 400−4000 cm^{-1}): 418(s), 435(s), 508(s), 554(s), 648(m), 672(s), 750(s), 900(s), 924(s), 966(vs), 1019(s), 1061(vs), 1087(vs), 1155(m), 1220(m), 1244(m), 1297(s), 1352(m), 1436(s), 1461(s), 1620(m), 2871(s), 2919(s), 3352(s).

$[Ni^{II}V^{IV}_6O_6\{(OCH_2CH_2)_2N(CH_2CH_2OH)\}_6]2Cl\cdot H_2O$ (7). The nickel derivative (**7**) was synthesized from a mixture of 0.0504 mmol of $[NH_4]_6[V_{10}O_{28}]\cdot 6H_2O$, 0.27 mmol of $NiCl_2\cdot 6H_2O$, 57.36 mmol of CH_3CN, 51.46 mmol of C_2H_5OH, and 1.3 mmol of $[C_2H_4OH]_3N$ sealed in a Teflon-lined Parr reaction vessel. The Parr vessel was heated in a Thermoline oven at 145 °C for 26 h. The reaction vessel was cooled to room temperature for 12 h. The brown solution was decanted, and the green crystals were washed with ethanol according to the procedure described for **1** to remove black and colorless impurities. The green crystals were air dried at room temperature, and any white crystalline impurity mixed with the green crystalline product was mechanically removed. Yield: 41.52% (based on vanadium). Anal. Calcd for $NiV_6O_{25}C_{36}H_{80}N_6Cl_2$: Ni, 4.10; V, 21.34; C, 30.19; H, 5.63; N, 5.87; Cl, 4.95. Found: Ni, 4.18; V, 21.41; C, 30.01; H, 5.67; N, 5.80; Cl, 5.31. Prominent IR bands (KBr pellet 400−4000 cm^{-1}): 442(s), 513(vs), 558(s), 670(vs), 749(vs), 900(s), 968(vs), 1081(s), 1041(s), 1059(s), 1087(vs), 1156(m), 1222(m), 1242(s), 1298(s), 1309(s), 1350(m), 1459(vs), 1437(vs), 1622(s), 2866(vs), 3383(vs).

Single-Crystal X-ray Diffraction. The single-crystal X-ray diffraction data for the crystals of the lithium, sodium, manganese, and iron derivatives (**1**, **2**, **4**, and **5**) were collected on a Bruker SMART CCD[23] diffractometer equipped with graphite-monochromatized Mo Kα radiation. The data were processed with SAINT Software,[24] and empirical absorption corrections were applied with SADABS.[25] All calculations were performed using the SHELXTL[26] package. X-ray powder diffraction patterns for **3**, **6**, and **7** were run on a Siemens D5000 powder XRD at room temperature between 5×bc and 80° 2θ at 3 s count for every 0.02×bc.

Results and Discussion

The solvothermal reactions of decavanadates with triethanolamine in the presence of heterometal salts in a mixed solvent media (CH_3OH/C_2H_5OH and CH_3CN) gave **1**−**7** in moderate to high yields. While only the best preparation methods that produced high-purity crystalline materials of the reported compounds in moderate to high yields are described here, a large number of reactions with varying reaction conditions (reactants, stoichiometry, reaction time, and temperature) have been carried out in each case to study the effect of reaction parameters on the formation of the products. Most of the compounds can be prepared under slightly different reaction stoichiometries, temperatures, and reaction times. The synthetic procedures described in the Experimental Section yielded fully reduced bright-colored crystalline materials that are very pleasant to look at. In each case the mother liquor that was stored at room temperature in a closed glass tube yielded only colorless organic materials—tetrabutylammonium or triethanol ammonium or ammonium salts.

Synthesis of the sodium derivative (**2**) is very sensitive to reaction conditions. A slight change in the stoichiometric ratio, time, or temperature reduces the yield of **2** drastically, producing a large amount of colorless crystalline impurity. In the preparation of $[MgV_6^{IV}O_6\{(OCH_2CH_2)_2NCH_2CH_2OH\}_6]2Br\cdot H_2O$ (**3**), when the chloride salt of magnesium was used instead of the bromide ($MgBr_2\cdot 6H_2O$), a mixture of light blue microcrystalline material and white impurity was obtained. The IR spectrum of the blue microcrystalline material was identical to that of crystalline **3**. Since separation of the blue material from white impurity was tedious, synthesis from the chloride salt is not reported here.

$[MnV_6^{IV}O_6\{(OCH_2CH_2)_2NCH_2CH_2OH\}_6]2Cl$ (**4**) could be prepared by three different methods using $MnCl_2\cdot 4H_2O$ and different sources of vanadates (ammonium decavanadate and tetrabutylammonium decavanadate). The method described here gives the best result (higher yield and purer material) as compared to two other methods[17a] in which tetrabutylammonium decavanadate was used as a reactant.

Bright green diamond-shaped X-ray diffraction quality crystals of $[FeV_6^{IV}O_6\{(OCH_2CH_2)_2NCH_2CH_2OH\}_6]2Cl$ (**5**) were first prepared in ~63% yield. By a systematic variation in the molar ratio of the reactants and reaction time, we were able to find optimum reaction conditions that increased the yield of this compound to above 90%. This high-yield method gives **5** in monophasic form but at the cost of crystal quality.

(23) *SMART*, version 4.210; Simens Analytical X-Ray Systems: Madison, WI 1997.

(24) *SAINT*, version 4.050; Simens Analytical X-Ray Systems: Madison, WI 1995.

(25) Sheldrick, G. M. *SADABS*; University of Gottingen: Gottingen, Germany 1997.

(26) Sheldrick, G. M. *SHELXTL*, version 5.1; Siemens Industrial Automation, Inc.: Madison, WI, 1995.

The thin blue crystals of $[CoV_6^{IV}O_6\{(OCH_2CH_2)_2NCH_2CH_2OH\}_6]2Cl\cdot H_2O$ (**6**) and the turquoise tetrahedral crystals of $[NiV_6^{IV}O_6\{(OCH_2CH_2)_2NCH_2CH_2OH\}_6]2Cl\cdot H_2O$ (**7**) were prepared readily. However, they were not suitable for single-crystal X-ray diffraction work.

Compounds **1**−**7** are highly colored, crystalline, and very stable in air at room temperature. This is also the case with the iron derivative $[Fe^{II}V_6^{IV}O_6\{(OCH_2CH_2)_2NCH_2CH_2OH\}_6]$-2Cl (**5**), which contains an Fe^{II} center, as previously reported.[17b] The reduced iron (Fe^{II}) center in **5** remains unoxidized in air at room temperature for a prolonged time.[27a] This indicates the remarkable robustness of the metallocyclic core in these clusters.

All of these compounds are highly soluble in water but insoluble in common organic solvents such as methanol, acetonitrile, ethanol, acetone, and methylene chloride. The aqueous solutions of **1**−**7** are brightly colored and stable over a remarkably wide pH range (2.5−11.8). The bright green and blue colors of crystals of **1**−**7** are characteristic of reduced compounds of vanadium. The results of manganometric titrations, which revealed the presence of $6V^{IV}$ sites per formula unit in each case, support this observation.

The FT-IR spectra of **1**−**7** exhibit similar features. The absorption patterns for the ligand and vanadium oxide framework are observed in the fingerprint regions, with slight variations in the position and intensity as a consequence of the presence of different heterometals in the framework. The strong absorption peaks present in the 970−961 and 943−953 cm^{-1} regions are assigned to the V=O stretch. The absorption peaks below 600 cm^{-1} are assigned to V−O−V and M−O symmetric and asymmetric stretches, respectively. The spectra for **1**−**7** show a very sharp band centered at 3301−3385 cm^{-1} assigned to the O−H stretch of the pendent CH_2CH_2OH group. For compounds **2**, **3**, **6**, and **7**, an additional medium or strong absorption band at 1617−1620 cm^{-1} is assigned to H−O−H bending of the solvate water molecules present in these materials.

The absorption bands due to the C−H stretch of the triethanolamine ligand are found in the region 2980−2850 cm^{-1}. The C−N stretch appears in the 1440−1431 cm^{-1} region, C−O stretching at 1088−1058 cm^{-1}, and $\delta_s CH_2$ in the 1460−1464 cm^{-1} region. The additional absorption bands in the 1400−1000 cm^{-1} region are due to in-plane O−H bending coupled with C−H wagging vibrations at 1420−1330 cm^{-1}, CH_2 twisting and wagging at 1350−1150 cm^{-1}, and out-of-plane C−H bending in the 749−450 cm^{-1} region.

The thermogravimetric analyses of **1**−**7** revealed weight-loss patterns that can be attributed to the loss of all of the C, H, and N atoms of the triethanolamine ligands, the anions, and the hydroxy oxygen atoms of the pendent arms in the 250−800 °C temperature range.[27b,c] The compounds with water of crystallization (compounds **2**, **3**, **6**, and **7**) begin losing weight at ∼40 °C. In each case the observed total weight loss corresponds well to the calculated weight loss. FT-IR spectra of the black residues left after the thermogravimetric experiments indicate the presence of mixed-metal vanadium oxide phases in the residue. These have not been characterized further.

Compounds **1**−**7** were prepared in the form of highly crystalline materials, and the crystal structures of four representative examples of this series, $[LiV_6^{IV}O_6\{(OCH_2CH_2)_2NCH_2CH_2OH\}_6]Cl\cdot LiCl$ **(1)** $[NaV^{IV}{}_6O_6\{(OCH_2CH_2)_2N(CH_2CH_2OH)\}_6]Cl\cdot H_2O$ (**2**), $[Mn^{II}V^{IV}{}_6O_6\{(OCH_2CH_2)_2N(CH_2CH_2OH)\}_6]2Cl$ (**4**), and $[Fe^{II}V_6^{IV}O_6\{(OCH_2CH_2)_2NCH_2CH_2OH\}_6]2Cl$ (**5**), were determined by complete single-crystal X-ray diffraction analysis. The crystals of compounds **3**, **6**, and **7** were found to be poorly X-ray diffracting and did not yield data sets suitable for complete single-crystal structure analyses. They were, however, studied by X-ray powder diffraction and a number of other characterization techniques.

Crystallographic data for **1**, **2**, **4**, and **5** are summarized in Table 1. Each of these compounds contains fully reduced cluster cations $[MV^{IV}{}_6O_6\{(OCH_2CH_2)_2N(CH_2CH_2OH)\}_6]^{n+}$ (**1**, M = Li^+, n =1; **2**, M = Na^+, n = 1; **4**, M = Mn^{2+}, n = 2; **5**, M = Fe^{2+}, n = 2) and chloride anions. Although these four cluster ions have three different crystallographic site symmetries, their overall configurations are essentially identical. In each case the cluster ion is composed of a fully reduced cyclic $\{MV_6N_6O_{18}\}$ (M = Li, Na, Mn, Fe) framework decorated with six triethanolamine ligands. Two arms of each of the triethanolamine ligands are coordinated to the metallacycle, and the third ligand arm projects outward from the hexagonal ring. Figure 1 shows a view of the cluster cation of **4.** Drawings of the other clusters have been deposited as Supporting Information. The $\{MV_6N_6O_{18}\}$ core in **1**, **2**, **4**, and **5** adopts the Anderson-type structure.[18,19a,20a] The cyclic core, shown in Figure 2, is comprised of a ring of six edge-sharing $\{VO_5N\}$ octahedra linked to the central $\{MO_6\}$ unit. The six vanadium atoms lie alternately on opposite sides of their mean plane, which contains the M^{n+} ion. Bond valence sum calculations indicate that none of the μ_2- and μ_3-oxo groups associated with the cyclic core are protonated. These results are consistent with the presence of six vanadium(IV) sites, as determined from the redox titrations, and with charge balance considerations.

(27) This was proved by redox titration and magnetic measurements on freshly prepared samples and samples of **5** that were exposed to air for 2, 4, and 12 weeks. (b) The thermogravimetric analysis on a sample of **1** showed a total weight loss of 53.5% between 249 and 800 °C. This corresponds with the calculated weight loss due to the removal of all the organics (C, H, and N) of the ligand, chloride ion, and six oxygen atoms from the pendent arms of triethanolamine molecules. The FT-IR of the black shiny residue gives absorption bands at 665, 625, and 450 cm^{-1}, indicating the presence of a vanadium oxide phase in the residue. Compounds **4** and **5** follow a similar weight-loss pattern.[27c] The thermal analysis on a sample of **2** showed a total weight loss of 52.84% between 38 and 800 °C. This corresponds to the calculated weight loss (54.7%) due to the loss of all organics (C, H, and N), chloride ion, solvated water, and six oxygen atoms from the pendent arms of triethanolamine ligands. Compounds **3**, **6**, and **7** show a similar weight-loss pattern.[27c] (c) Thermogravimetric analysis of **3** gave a total weight loss of 57.59% between 40 and 800 °C, corresponding to a calculated weight loss of 58.47%. Thermal analysis of **4** indicated a total weight loss of 47.3% between 250 and 700 °C, corresponding to a calculated weight loss of 47.6%. Thermogravimetric analysis on **5** gave a total weight loss of 54.7% between 224 and 700 °C, corresponding to a calculated weight loss of 53.984%. Thermogravimetric analysis of **6** indicated a total weight loss of 56.49% between 40 and 800 °C, corresponding to a calculated weight loss of 54.45%. Thermal analysis of **7** gave a total weight loss of 55.04% between 43 and 800 °C, corresponding to a calculated weight loss of 54.46%.

Table 1. Crystallographic Data for $[LiV_6^{IV}O_6\{(OCH_2CH_2)_2NCH_2CH_2OH\}_6]Cl\cdot LiCl$ (**1**), $[NaV_6^{IV}O_6\{(OCH_2CH_2)_2NCH_2CH_2OH\}_6]Cl\cdot H_2O$ (**2**), $[Mn^{II}V_6^{IV}O_6\{(OCH_2CH_2)_2NCH_2CH_2OH\}_6]2Cl$ (**4**), and $[Fe^{II}V_6^{IV}O_6\{(OCH_2CH_2)_2NCH_2CH_2OH\}_6]2Cl$ (**5**)

	1	**2**	**4**	**5**
empirical formula	$C_{36}H_{78}Cl_2N_6Li_2O_{24}V_6$	$C_{36}H_{80}ClN_6NaO_{25}V_6$	$C_{36}H_{78}Cl_2N_6MnO_{24}V_6$	$C_{36}H_{78}Cl_2N_6FeO_{24}V_6$
formula weight	1369.46	1361.14	1410.52	1411.43
cryst syst	trigonal	triclinic	monoclinic	monoclinic
space group	$R\bar{3}$	$P\bar{1}$	$P2_1$	$P2_1$
a (Å)	13.7185(3)	11.1817(5)	11.2208 (5)	11.3057 (7)
b (Å)	13.7185(3)	12.1612(5)	21.5041 (9)	21.4372 (13)
c (Å)	24.8899(8)	21.5979(10)	11.8126(5)	11.8167(7)
α (deg)	90	75.8210(10)	90	90
β (deg)	90	78.8270(10)	111.2680	111.4170
γ (deg)	120	71.1400(10)	90	90
V (Å^3)	4056.6(2)	2673.5(2)	2656.2(2)	2666.2(3)
Z	3	2	2	2
T (K)	173(2)	183(2)	178(2)	173(2)
ρ_{cal} (Mg.m^{-3})	1.673	1.691	1.764	1.764
μ (mm^{-1})	1.177	1.151	1.426	1.758
radiation λ (Å)	0.710 73	0.710 73	0.710 73	0.710 73
no. of reflections	2212	12 474	12 675	12 593
no. of parameters	118	664	663	677
R_1 (F_0)[a] (all data)	0.0736	0.0497	0.0478	0.1077
wR_2 (F_0^2)[b]	0.2027	0.1186	0.1227	0.2300
GOF	1.290	1.036	1.024	1.050

[a] $R1 = \sum||F_o| - |F_c||/\sum|F_o|$. [b] $wR2 = [\sum[w(F_o^2 - F_c^2)^2]/\sum[w(F_o^2)^2]]^{1/2}$.

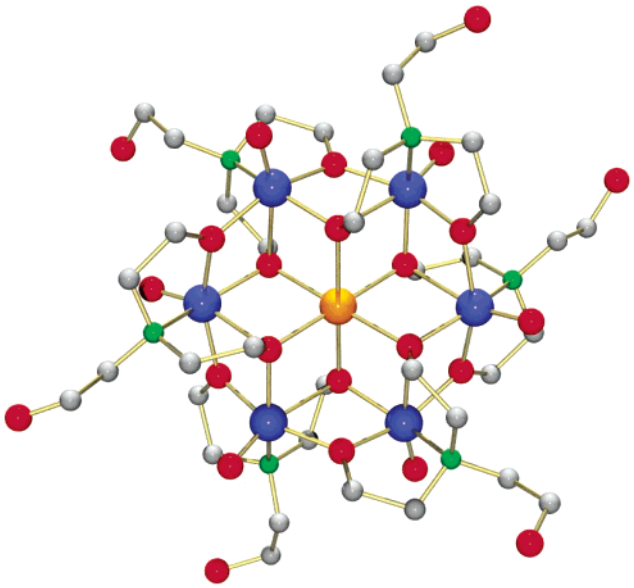

Figure 1. View of the cluster cation $[Mn^{II}V^{IV}_6O_6\{(OCH_2CH_2)_2N(CH_2CH_2OH)\}_6]^{2+}$ present in the crystals of $[Mn^{II}V^{IV}_6O_6\{(OCH_2CH_2)_2N(CH_2CH_2OH)\}_6]2Cl$ (**4**).

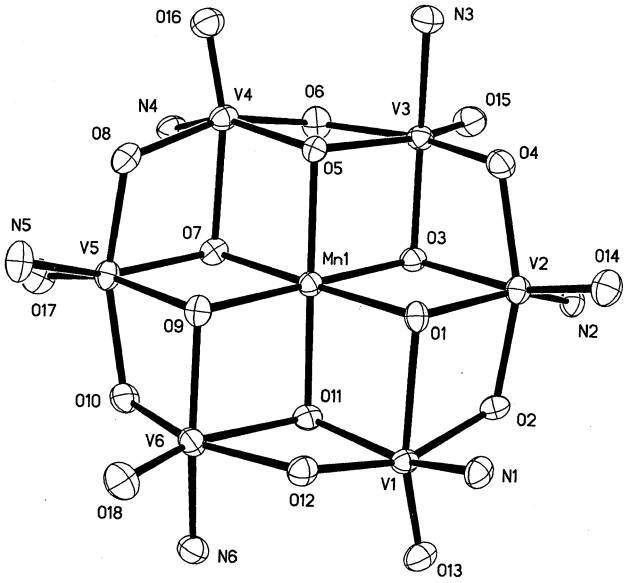

Figure 2. View of the cyclic metal oxide framework $\{MnV_6N_6O_{18}\}$ showing the metal atoms and their coordination environments in the cluster cation species in $[Mn^{II}V^{IV}_6O_6\{(OCH_2CH_2)_2N(CH_2CH_2OH)\}_6]2Cl$ (**4**).

Each of the six vanadium atoms in the core is bound to a terminal oxygen atom as well as to five atoms from the triethanolamine ligands—a nitrogen donor atom, two μ_2-O atoms, and two μ_3-O atoms. Each adjacent pair of vanadium atoms around the ring is linked by one μ_2-O atom and one μ_3-O atom; the third bond of each triply bridging oxygen atom is to the central metal ion. Two arms of each of the six triethanolamine ligands are coordinated to the metallacycle, and the third arm projects outward from the hexagonal ring. In some cases the pendant arms are disordered. The free hydroxy groups of these arms participate in hydrogen bonding to the chloride ions and, in the case of **2**, to the solvate water molecule. A view of the unit cell contents of **4**, projected down the *a*-axis, is given in Figure 3, which shows the relationship between the cations and anions in **4**.

Geometrical details of the central cores of **1**, **2**, **4**, and **5** are tabulated in Table 2, and complete listings of bond distances and angles may be found in the deposited cif files as Supporting Information. Although the M−O distances to the central atom span a range of almost 0.15 Å, the overall sizes of the cations and most of their structural details are closely similar. The primary variations associated with longer M−O distances are larger O(μ_3)−V−O(μ_3) and V−O(μ_3)−V angles. The ability of the $\{MV_6N_6O_{18}\}$ framework to accommodate central ions varying in size and charge documents its remarkable flexibility.

Although the cluster ions of **1**, **2**, **4**, and **5** have the same overall structure, these four compounds crystallize in three different space groups, and the cations have three different crystallographic symmetries. Compounds **4** (M = Mn^{2+}) and

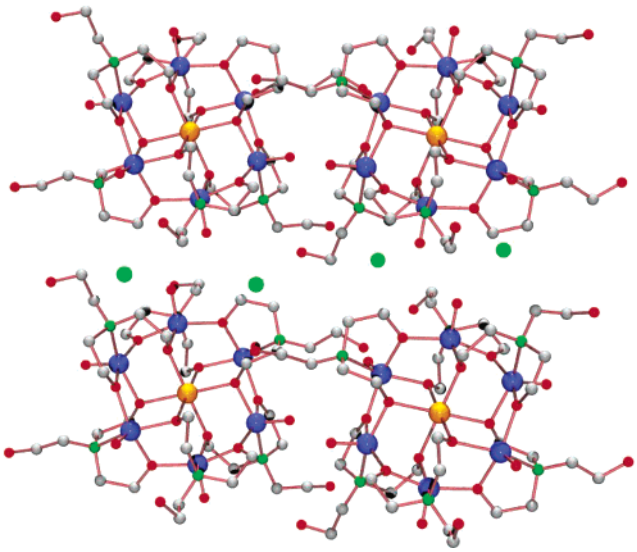

Figure 3. Unit cell contents of the crystals of $[Mn^{II}V^{IV}{}_6O_6\{(OCH_2CH_2)_2N(CH_2CH_2OH)\}_6]2Cl$ (**4**) projected down the *a*-axis, showing the relationship between the cluster cations and chloride anions.

Table 2. Mean Dimensions (Å, deg) of the $\{MV_6N_6O_{18}\}^{n+}$ Cages in **1**, **2**, **4**, and **5**

	1 (M = Li)	**2** (M = Na)	**4** (M = Mn)	**5** (M = Fe)
V (Å^3)/cation[a]	1352	1336	1328	1333
M−O	2.200(3)[b]	2.291(2)	2.184(3)	2.147(5)
V−O (terminal)	1.615(4)	1.612(2)	1.596(4)	1.647(7)
V−O(μ_2)[c]	1.937(4)	1.953(2)	1.952(4)	1.956(6)
	2.021(4)	2.041(2)	2.018(4)	2.014(6)
V−O(μ_3)	2.004(3)	1.997(2)	2.039(4)	2.045(5)
	2.195(3)	2.195(2)	2.278(4)	2.258(5)
V−N	2.178(4)	2.207(2)	2.170(4)	2.169(7)
O−M−O	80.23(11)	79.32(6)	80.95(13)	80.85(20)
	99.77(11)	100.68(6)	99.05(13)	99.15(19)
	180[d]	180[d]	179.39(16)	179.49(22)
V−O(μ_2)−V	109.87(16)	110.00(9)	112.49(17)	111.63(26)
V−O(μ_3)−V	100.89(14)	102.52(8)	99.58(14)	99.40(21)
M−O−V	100.31(14)	98.65(7)	102.21(14)	102.65(22)
	94.60(13)	93.16(7)	94.92(13)	95.96(20)
O(μ_2)−V−O(μ_2)	160.47(17)	159.10(8)	158.67(16)	159.94(23)
O(μ_3)−V−O(μ_2)	71.43(13)	70.50(7)	70.37(14)	71.20(20)
		76.59(8)	76.98(14)	77.12(22)
	89.42(14)	89.96(7)	88.63(14)	89.03(21)
		95.21(8)	95.84(15)	95.88(22)
O(μ_3)−V−O(μ_3)	84.82(19)	88.86(7)	81.89(13)	80.50(20)

[a] Calculated as the unit cell volume divided by the number of cluster cations per cell. [b] All tabulated standard deviations are the average esd's of an *individual* measurement. [c] Where distances of a given type cluster about more than one distinctly different average value, each of the mean values is listed. [d] Exact value, constrained by symmetry.

5 (M = Fe^{2+}) crystallize in space group $P2_1$, which imposes no symmetry on the cation. The space group of compound **1** (M = Li^+) is $R\bar{3}$, and the cation has $\bar{3}$ crystallographic symmetry. Compound **2** (M = Na^+) crystallizes in space group $P\bar{1}$, and the cations are centrosymmetric, with two half cations comprising the asymmetric unit. Differences in chloride content and solvation, and possibly also small differences in cation dimensions, presumably contribute to these variations.

The crystals of **3**, **6**, and **7** were not of sufficient quality for single-crystal X-ray studies. Their X-ray powder diffraction patterns in combination with other analytical data (from elemental analysis, FT-IR, TGA, manganometric titrations, and magnetic susceptibility measurement) are consistent with the presence of cluster cations $[M^{II}V^{IV}{}_6O_6\{(OCH_2CH_2)_2N(CH_2CH_2OH)\}_6]^{n+}$ (**3**, $M^{II} = Mg^{2+}$, $n = 2$; **6**, $M^{II} = Co^{2+}$, $n = 2$; **7**, $M^{II} = Ni^{2+}$, $n = 2$) which have structures analogous to the clusters present in **1**, **2**, **4**, and **5**.

Table 3. Effective Magnetic Moments of $[LiV^{IV}{}_6O_6\{(OCH_2CH_2)_2N(CH_2CH_2OH)\}_6]Cl\cdot LiCl$ (**1**), $[NaV^{IV}{}_6O_6\{(OCH_2CH_2)_2N(CH_2CH_2OH)\}_6]Cl\cdot H_2O$ (**2**), $[MgV^{IV}{}_6O_6\{(OCH_2CH_2)_2N(CH_2CH_2OH)\}_6]2Br\cdot H_2O$ (**3**), $[Mn^{II}V^{IV}{}_6O_6\{(OCH_2CH_2)_2N(CH_2CH_2OH)\}_6]2Cl$ (**4**), $[Fe^{II}V_6O_6\{(OCH_2CH_2)_2N(CH_2CH_2OH)\}_6]2Cl$ (**5**), $[Co^{II}V^{IV}{}_6O_6\{(OCH_2CH_2)_2N(CH_2CH_2OH)\}_6]2Cl\cdot H_2O$ (**6**), and $[Ni^{II}V^{IV}{}_6O_6\{(OCH_2CH_2)_2N(CH_2CH_2OH)\}_6]2Cl\cdot H_2O$ (**7**)

compound	μ_{eff} at 300 K (μ_B)	μ_{eff} expected for noninteracting spins (μ_B)
1	4.33	4.14−4.24
2	4.29	4.14−4.24
3	3.78	3.77−3.87
4	8.81	7.20−7.35
5	7.93	6.65−6.95
6	7.79	6.10−6.65
7	6.63	5.00−5.45

The $\{V_6O_{12}\}$ ring in **1**−**7** may be regarded as a hexadentate ligand to the metal M, forming $\{MV_6O_{12}\}$ chelates. The cavity in the oxometallic ligand exhibits remarkable flexibility to accommodate a variety of metal ions M^{n+} (M = Li, Na, Mg, Mn, Fe, Co, Ni) of different sizes, which could possibly be a consequence of the presence of a fully reduced metallocyclic core. An earlier report[28] shows a fully oxidized species $[NaV_6O_6\{(OCH_2CH_2)_2NCH_2CH_2OH\}_6]_2S_6\cdot 2CH_3OH$ where sodium ion is encapsulated in the cavity defined by the anionic hexavanadate core. Other examples of functionalized hexavanadate clusters[29−31] are those incorporating tris(hydroxymethyl)alkane ligands in a reduced $\{V_6O_{19}\}$ core that has a Lindquist-type structure.[32,33]

The fully reduced hexavanadate cores in **1**−**7**, containing six spins from $6d^1$ (V^{IV}) centers, act as ligands for the encapsulated M^{n+} (M^{n+} = Li^+, Na^+, Mg^{2+}, Mn^{2+}, Fe^{2+}, Co^{2+}, Ni^{2+}) centers with different spins. This leads to interesting magnetic properties as revealed by the variable-temperature magnetic susceptibility measurements. The effective magnetic moments (μ_{eff}) of **1**−**7** and the corresponding expected μ_{eff} for noninteracting spins are given in Table 3. Magnetic susceptibility χ data for $[LiV_6O_6\{(OCH_2CH_2)_2N(CH_2CH_2OH)\}_6]Cl\cdot LiCl$ (**1**), presented in Figure 4, shows that the effective moment $\mu_{eff} = \sqrt{8\chi_0 T}$ ($\chi_0 = \chi -$ TI, where TI is a temperature independent contribution, i.e., diamagnetism + temperature-independent paramagnetism) of the compound increases with decreasing temperature. This indicates the presence of ferromagnetic interactions. The effective magnetic moment at 300 K (4.33 μ_B) is close to the expected value for six noninteracting spins $S = {}^1/_2$, while the moment at 2 K (7.04 μ_B) is characteristic for $S = 3$,

(28) Chen, Y.; Liu, Q.; Deng, Y.; Zhu, H.; Chen, C.; Fan, H.; Liao, D.; Gao, E. *Inorg. Chem.* **2001**, *40*, 3725. (b) Thomas, C.; Li, P.; Zheng, C.; Huang, K. *Chem. Commun.* **1986**, 1597.
(29) Khan, M. I.; Chen, Q.; Zubieta, J. *Inorg. Chem.* **1992**, *31*, 1556.
(30) Khan, M. I.; Chen, Q.; Hope, H.; Parkin, S.; O'Connor, C. J.; Zubieta, J. *Inorg. Chem.* **1993**, *32*, 2929.
(31) Chen, Q.; Goshorn, D.; Scholes, C.; Tan, X.; Zubieta, J. *J. Am. Chem. Soc.* **1992**, *114*, 4667.
(32) Lindqvist, I. *Ark. Kemi.* **1952**, *5*, 247.
(33) Kepert D. L. *Inorg. Chem.* **1969**, *8*, 1556.

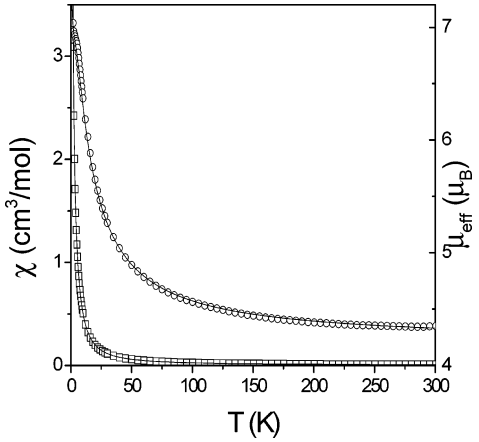

Figure 4. Magnetic susceptibility χ (□) and effective magnetic moment μ_{eff} (○) of the lithium derivative (**1**) over temperature *T*. The line drawn through the data is the fit to the Heisenberg six-atom ring model.

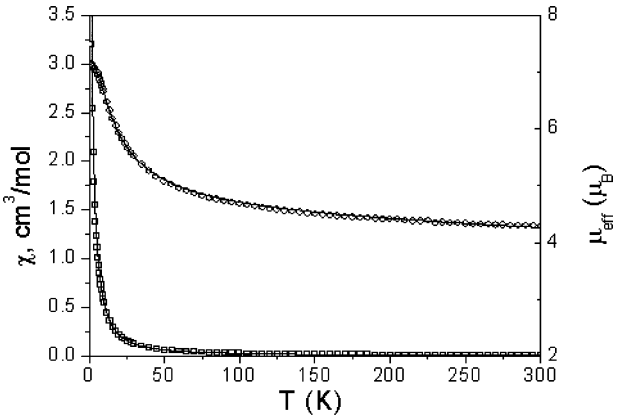

Figure 5. Dependence of the magnetic susceptibility χ (□) and effective magnetic moment μ_{eff} (○) of the sodium derivative (**2**) on temperature *T*. The line drawn through the data is the fit to the Heisenberg six-atom ring model.

which results from the ferromagnetic interactions between these spins. The experimental results have been described using the Heisenberg six-atom ring model ($S = {}^1/_2$).[22] The Hamiltonian is

$$H = -2J\sum_{i=1}^{6} \boldsymbol{S_i S_{i+1}} - g\mu_B H \cdot \sum_{i=1}^{6} S_i, \qquad \text{(I)}$$

where S_7 is defined as S_1. The energy of the levels for this system were obtained in ref 22b. These values were substituted in Van Vleck's equation, and the obtained expression for magnetic susceptibility was used to fit the experimental data. The calculated susceptibility χ has been corrected for intermolecular exchange interaction zJ'

$$\chi' = \frac{\chi_0}{1 - (2zJ'/N_A g^2 \mu_B{}^2)\chi} \qquad \text{(II)}$$

The best fit was $g = 1.95$, $J = 19.0$ K, $zJ' = 0.015$ K, and TI $= -0.00065$ cm^3/mol.

The effective magnetic moment of $[NaV_6O_6\{(OCH_2CH_2)_2N(CH_2CH_2OH)\}_6]Cl\cdot H_2O$ (**2**) (Figure 5) at 300 K is 4.29 μ_B, which again is attributed to six noninteracting spins $S = {}^1/_2$ of six vanadium atoms in the +4 (V^{IV}) state. The

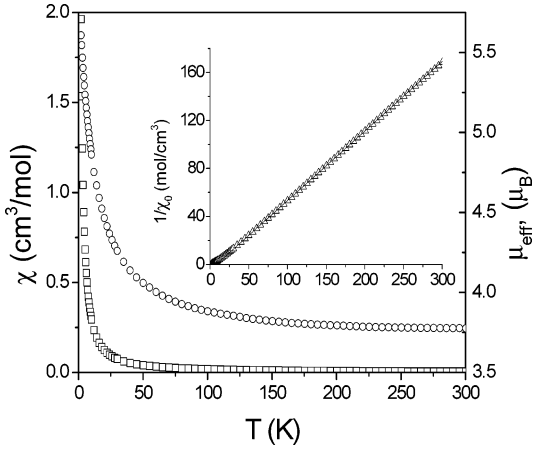

Figure 6. Magnetic susceptibility χ (□), effective magnetic moment μ_{eff} (○), and the reverse susceptibility $1/\chi_0$ (△) of the magnesium compound (**3**) over temperature *T*. The line drawn through the data is the fit to the Curie−Weiss law.

effective magnetic moment increases with decreasing temperature, indicating the presence of ferromagnetic interactions. The moment at 2 K (7.13 μ_B) is characteristic for $S = 3$, which results from the ferromagnetic interaction between these spins. The experimental results were best described using the Heisenberg six-atom ring model ($S = {}^1/_2$). The Hamiltonian used is given in eq I. The best fit was $g = 2.04$, $J = 19.6$ K, and TIP $= -0.001$.

Magnetic susceptibility data for $[MgV_6O_6\{(OCH_2CH_2)_2N(CH_2CH_2OH)\}_6]2Br\cdot H_2O$ (**3**) is shown in Figure 6. The μ_{eff} value increases with decreasing temperature, indicating the presence of ferromagnetic interactions. The effective magnetic moment at 300 K (3.78 μ_B) is close to the expected value for five noninteracting spins $S = {}^1/_2$ (1.69 μ_B per magnetic ion), while the moment at 2 K (5.60 μ_B) is characteristic for $S = {}^5/_2$. Unfortunately the lack of information about spin configuration does not allow a precise description of such a system. The high-temperature data were extrapolated to Curie−Weiss law

$$\chi = \chi_0 + TI = \frac{C}{T - \theta} + \text{TI}$$

The best fit was $C = 1.73$ cm^{3}K/mol, $\theta = -8.1$ K, and TI $= -0.00076$ cm^3/mol.

Figures 7 and 8 show the temperature-dependent magnetic susceptibilities and magnetic moment data for $[MnV_6O_6\{(OCH_2CH_2)_2N(CH_2CH_2OH)\}_6]2Cl$ (**4**) and $[Fe^{II}V_6{}^{IV}O_6\{(OCH_2CH_2)_2NCH_2CH_2OH\}_6]2Cl$ (**5**), respectively. The μ_{eff} values (8.81μ_B for **4** and 7.93μ_B for **5**) at 300 K are much higher than the expected values (given in Table 3) for noninteracting spins, indicating the presence of strong ferromagnetic intramolecular exchange interactions in both cases. The magnetic moment of **4** decreases with a decrease in temperature. As a consequence of the strong ferromagnetic intramolecular exchange interaction in **5**, there is an increase in the effective magnetic moment with decreasing temperature to 15 K. However, at liquid helium temperature the effective magnetic moment of **5** drops below the room-temperature (300 K) value, probably as a consequence of zero-field splitting.

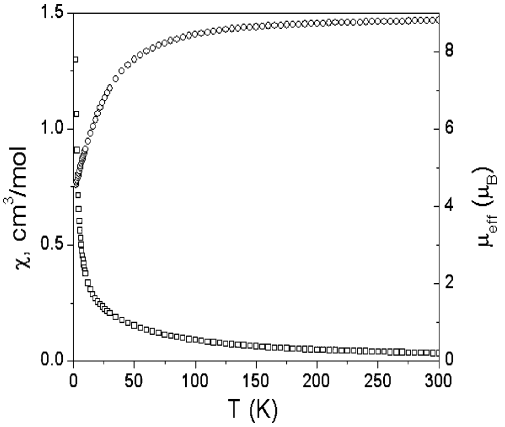

Figure 7. Magnetic susceptibility χ (□) and effective magnetic moment μ_{eff} (○) of the manganese derivative (**4**) over temperature *T*.

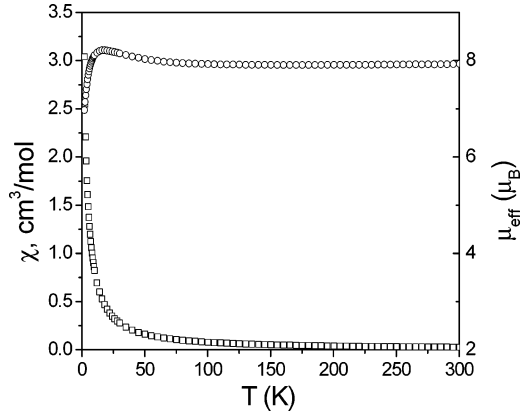

Figure 8. Dependences of the magnetic susceptibility χ (□) and effective magnetic moment μ_{eff} (○) of the iron derivative (**5**) on temperature *T*.

The effective magnetic moments of $[CoV_6O_6\{(OCH_2CH_2)_2N(CH_2CH_2OH)\}_6]2Cl\cdot H_2O$ (**6**) and $[NiV_6O_6\{(OCH_2CH_2)_2N(CH_2CH_2OH)\}_6]2Cl\cdot H_2O$ (**7**) at 300 K, 7.79 and 6.43 μ_B, respectively, are also much higher than the expected value for noninteracting spins, indicating the presence of a rather strong ferromagnetic intramolecular exchange interaction. In the case of **6** the decrease in the effective magnetic moment with decreasing temperature indicates a strong influence of the zero-field splitting. The possibility of intermolecular exchange should be taken into account also, but in this case it is difficult to separate the contributions of these mechanisms (Figure 9). In the case of **7** the increase in the effective moment with decreasing temperature up to 35 K is also a result of strong ferromagnetic intramolecular exchange interaction. At liquid He temperature the effective magnetic moments drop below the values at 300 K, indicating an antiferromagnetic intermolecular exchange (Figure 10).

Conclusion

The series of compounds described here constitutes the first examples of fully reduced hexavanadium-based cationic clusters containing metallocyclic cores exhibiting the Anderson-type structure and functionalized with organic ligands. They also represent important members of magnetic clusters that can have potential application in the emerging field of molecular magnetism and in the controlled synthesis of magnetic materials.

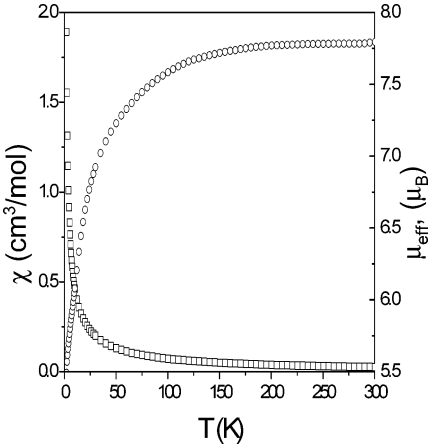

Figure 9. Magnetic susceptibility χ (□) and effective magnetic moment μ_{eff} (○) of the cobalt compound (**6**) over temperature *T*.

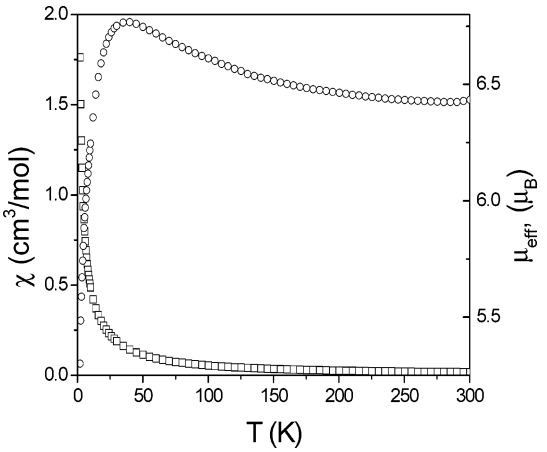

Figure 10. Magnetic susceptibility χ (□) and effective magnetic moment μ_{eff} (○) of the nickel compound (**6**) over temperature *T*.

The cavity defined by the hexametalate $\{V_6O_{12}\}$ ring in these clusters has shown remarkable flexibility to encapsulate a variety of magnetic and nonmagnetic ions of different sizes. The hexametalate ring contains six d^1 spins and acts as a ligand for the encapsulated M^{n+} ($M^{n+} = Li^+$, Na^+, Mg^{2+}, Mn^{2+}, Fe^{2+}, Co^{2+}, Ni^{2+}) centers with different spins. It is clear now that the cavity can encapsulate other magnetic ions of appropriate sizes. This can pave the way for the synthesis and characterization of other members of this series and allows for modifications in the magnetic behavior of these compounds. This not only enables comparison of the magnetic behavior of different derivatives containing the $\{MV_6O_{12}\}$ core but also provides an opportunity to study the interaction of six spins due to six V^{IV} centers with the encapsulated (M^{n+}) species. Moreover, the pendant $\{-CH_2OH\}$ arms of the triethanolamine ligands on **1**−**7** are potential binding sites, making these magnetic clusters promising building blocks for constructing supramolecular structures and extended structure magnetic solids.

Although the exact reaction pathway and intermediates are not yet established, it is clear that under solventothermal conditions the decavanadate unit defragments and undergoes a "reduction−reconstruction" self-assembly process incorporating the oxygen atoms of the triethanolamine ligand into the cyclic metal oxide framework. During self-assembly the

two arms of each triethanolamine are incorporated as μ_2 and μ_3 bridging alkoxide ligands in the fully reduced cyclic hexametallic core of the Anderson-type structure in these compounds. Furthermore, this work demonstrates the potential of a soft solvothermal synthetic method for the preparation of inorganic−organic hybrid materials with desirable magnetic, optical, and catalytic properties.[34]

Acknowledgment. This work was supported by a grant (to M.I.K.) from the American Chemical Society's Petroleum Research Fund (ACS-PRF#35591-AC5) and NSF (CHE-0210354). C.J.O. and V.G. gratefully acknowledge the support from the Louisiana Board of Regents contract no. NSF/LEQSF (2001-04)-RII-03.

(34) Detailed study of the catalytic and optical properties is in progress.

Supporting Information Available: X-ray crystallographic files in CIF format for the structure determinations of $[LiV_6^{IV}O_6\{(OCH_2CH_2)_2NCH_2CH_2OH\}_6]Cl\cdot LiCl$ **(1),** $[NaV^{IV}_6O_6\{(OCH_2CH_2)_2N(CH_2CH_2OH)\}_6]Cl\cdot H_2O$ (**2**), $[Mn^{II}V^{IV}_6O_6\{(OCH_2CH_2)_2N(CH_2CH_2OH)\}_6]$-2Cl (**4**), and $[Fe^{II}V_6^{IV}O_6\{(OCH_2CH_2)_2NCH_2CH_2OH\}_6]2Cl$ (**5**). This material is available free of charge via the Internet at http://pubs.acs.org. Details of the crystallographic data have been deposited (CCDC reference number: **1**, CCDC 236397; **2**, CCDC 236396; **4**, CCDC 196923; **5**, CCDC 216908) with the Cambridge Crystallographic Data Center, 12 Union Road, Cambridge, CB21EZ, UK (deposit@CCDC.cam.ac.uk).

IC049417M